Acoustic Illusion Using Materials with Isotropic and Positive Parameters

Yichao Liu[1] and Sailing He[1,2,*]

[1] *National Engineering Research Center for Optical Instruments, Centre for Optical and Electromagnetic Research, JORCEP, College of Optical Science and Engineering, East Building #5, Zijingang Campus, Zhejiang University, Hangzhou 310058, China*

[2] *Department of Electromagnetic Engineering, School of Electrical Engineering, Royal Institute of Technology (KTH), S-100 44 Stockholm, Sweden*

(Received 2 July 2018; revised manuscript received 9 October 2018; published 14 December 2018)

Acoustic illusion devices are usually designed using transformation optics. An alternate method is proposed to achieve acoustic illusions without external devices by elaborately manipulating the acoustic scattering potential of an object. The proposed method is more of a "cosmetic operation" for an object, which modifies the scattered acoustic pressure distribution of the object to mimic another object by exchanging their scattering potentials in two symmetrical areas in the wave vector domain. The advantage of this method is the simplicity of material parameters: only positive isotropic mass density and bulk modulus are required, which is impossible with the conventional method of using transformation optics due to the complex material requirements (anisotropic and negative index parameters).

DOI: 10.1103/PhysRevApplied.10.064036

I. INTRODUCTION

Illusion effects, usually found in rare natural phenomena, have long attracted people's attention and played a major role in science fiction and movies. Artificial illusion effects are referred to by some people as techniques that can make one object conceal itself or resemble another object by giving a detector some tricking signals. This technique stayed at the conceptual level until transformation optics [1,2] (TO) was proposed, especially the pioneer works in illusion optics and complementary media [3–5], which show a possible method that can be used to design conceptual illusion devices using metamaterials. TO is a mathematical tool to calculate the electromagnetic parameters of one device with predefined functions by relating the material parameters and the spatial geometry based on a invariance of Maxwell's equations. Many optical devices have been designed using TO, such as invisibility cloaks [6–12], superlenses [13–15], concentrators [16–18], rotators [16,19], illusion devices [20–23], etc. See references [24–26] for a review. TO has also been used to design various acoustic devices, such as acoustic invisibility cloaks [27–29], acoustic concentrators [30], acoustic rotators [31], and acoustic illusions [32,33]. The key idea of TO is to design illusion devices (including acoustic and optical illusions) using complementary media to cancel the scattering of the original object and give the detector the scattering pattern of a different object. However, illusion devices designed using TO present many difficulties in real implementations because the essential "superlens" part requires some negative index metamaterials.

In addition to the method of TO, there are some other mechanics that can be used to produce acoustic illusions, and the most intuitive case is for a synthesized acoustic signal (containing different voices within different frequency ranges), which causes different people to hear different voices. This is because the ears of different people act as acoustic filters with different passbands. Here, instead of manipulating acoustic signals in the frequency domain, we modify the material parameters (mass density or bulk modulus) as little as possible in the wave vector domain to change the acoustic scattering potential for acoustic illusions. There are also other illusion and cloaking methods for acoustic waves, such as scattering cancellation [34–36] and Fabry-Pérot resonance [37]. An alternate way to artificially manipulate electromagnetic (em) waves was proposed in 2015 by using spatial Kramers–Kronig (KK) media [38], followed by experimental demonstration [39,40] to show a perfect absorber. A similar method has been adopted for cloaking devices [41], although no similar concept has been proposed for acoustic waves. Here, we propose a method of modifying materials in a wave vector space by deriving the related theory directly in an acoustic wave equation (for ideal fluids) for illusion. Note that one advantage of our method is that the material could have no gain or loss, which simplifies the material parameters.

*sailing@kth.se

II. THEORY

Now we show the design method for acoustic illusions. Consider the two-dimensional case. When the material parameters (mass density and bulk modulus) have no drastic change, the acoustic wave equation is given by

$$\nabla^2 p(\boldsymbol{\rho}) + k_0^2 \gamma_\rho \gamma_\kappa p(\boldsymbol{\rho}) = 0, \tag{1}$$

where $p(\boldsymbol{\rho})$ is the total acoustic pressure, $\boldsymbol{\rho}$ is the position vector, k_0 is the wave vector in the background material, and γ_ρ, γ_κ are the relative mass density and relative compressibility coefficient (reciprocal of the relative bulk modulus $\gamma_\kappa = 1/\kappa_r$) with respect to a reference background, respectively, i.e., $\gamma_\rho = \rho/\rho_0$, $\kappa_r = \kappa/\kappa_0$ with ρ andκ and ρ_0 andκ_0 the mass density and bulk modulus of the material and background, respectively. We can rewrite the above equation as

$$\nabla^2 p(\boldsymbol{\rho}) + k_0^2 p(\boldsymbol{\rho}) = -k_0^2 V(\boldsymbol{\rho}) p(\boldsymbol{\rho}), \tag{2}$$

where $V(\boldsymbol{\rho})$ represents the acoustic scattering potential and is defined by

$$V(\boldsymbol{\rho}) = \gamma_\rho \gamma_\kappa - 1. \tag{3}$$

Assuming that the incident acoustic wave is a plane wave $p_i(\boldsymbol{\rho}) = e^{i\mathbf{k}_i \cdot \boldsymbol{\rho}}$ with an incident wave vector of $\mathbf{k}_i$, the scattered wave, $p_s(\boldsymbol{\rho}) = p(\boldsymbol{\rho}) - p_i(\boldsymbol{\rho})$, can be calculated using Green's function

$$p_s(\boldsymbol{\rho}) = \int_S k_0^2 V(\boldsymbol{\rho}') p(\boldsymbol{\rho}') g(\boldsymbol{\rho} - \boldsymbol{\rho}') d^2\rho', \tag{4}$$

where $g(\boldsymbol{\rho} - \boldsymbol{\rho}') = (i/4) H_0^{(1)}(k_0|\boldsymbol{\rho} - \boldsymbol{\rho}'|)$ denotes the two-dimensional Green's function.

Now we simplify the above equation using the Born approximation, i.e., using $p_i(\boldsymbol{\rho}')$ to replace $p(\boldsymbol{\rho}')$ in Eq. (4), and the far field approximation

$$H_0^{(1)}(k_0|\boldsymbol{\rho} - \boldsymbol{\rho}'|) \approx \sqrt{\frac{2}{i\pi k_0 |\boldsymbol{\rho} - \boldsymbol{\rho}'|}} e^{ik_0 \cdot |\boldsymbol{\rho} - \boldsymbol{\rho}'|}$$
$$\approx \sqrt{\frac{2}{i\pi k_0 \rho}} e^{i\mathbf{k_s} \cdot (\boldsymbol{\rho} - \boldsymbol{\rho}')}, \tag{5}$$

where $\mathbf{k_s}$ denotes the scattered wave vector. Then the scattered wave can be expressed as

$$p_s(\boldsymbol{\rho}) \approx k_0^2 \sqrt{\frac{i}{8k_0\pi\rho}} e^{i\mathbf{k}_s \cdot \boldsymbol{\rho}} \int_S V(\boldsymbol{\rho}') e^{i(\mathbf{k}_i - \mathbf{k}_s) \cdot \boldsymbol{\rho}'} d^2\rho'. \tag{6}$$

From the above equation, we find the scattered wave is a cylindrical wave and the amplitude is determined by $f(\mathbf{k}_i, \mathbf{k}_s) = \int_S V(\boldsymbol{\rho}') e^{i(\mathbf{k}_i - \mathbf{k}_s) \cdot \boldsymbol{\rho}'} d^2\rho'$. We know the Fourier transformation of the scattering potential is

$$V(\mathbf{k}) = \int_S V(\boldsymbol{\rho}) e^{-i\mathbf{k} \cdot \boldsymbol{\rho}} d^2\rho. \tag{7}$$

Therefore,

$$f(\mathbf{k}_i, \mathbf{k}_s) = V(\mathbf{k}_s - \mathbf{k}_i). \tag{8}$$

We can see the amplitude of the far-field scattered wave is associated with the Fourier components of the scattering potential. Therefore, we can control the scattered acoustic wave by modifying the relative mass density and bulk modulus (the scattering potential) in the wave vector domain to create illusion effects.

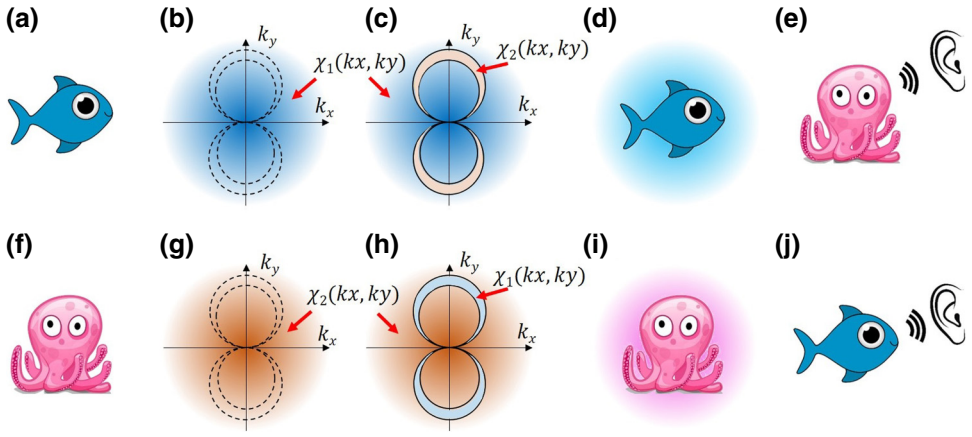

FIG. 1. Schematic diagram of acoustic illusions by modifying the acoustic scattering potential. The original two objects are (a) a fish and (f) a squid. (b),(g) are the Fourier transformations of the acoustic scattering potentials, denoted as $V_1(k_x, k_y)$ and $V_2(k_x, k_y)$ in the wave vector domain. The two crescent regions with dotted lines represent the scattering amplitudes with two incident directions $\mathbf{k}_0$, $-\mathbf{k}_0$, and within a wavelength band of $2\pi/k_{i1} \sim 2\pi/k_{i0}$. By exchanging the crescent regions in (b),(g), the acoustic scattering potentials in the wave vector domain are changed to (c),(h). The corresponding scattering potentials in the space domain are (d),(i). (e),(j) are the illusions when a detector/ear detects the acoustic pressure.

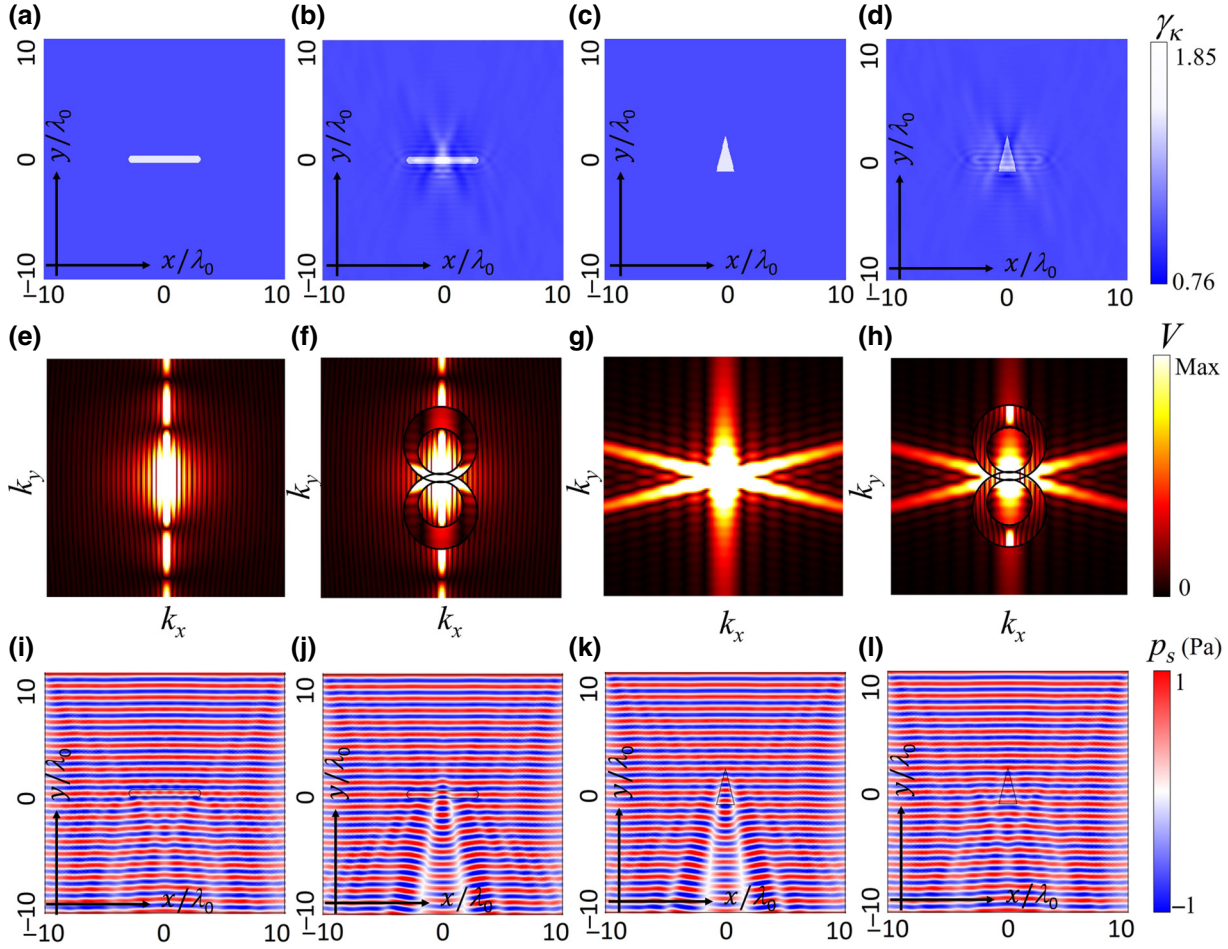

FIG. 2. Changing one object into another object. The relative compressibility coefficient of (a) the original capsule shape, (b) the modified capsule shape, (c) the original isosceles triangle, and (d) the modified isosceles triangle. (e)–(h) The corresponding acoustic scattering potentials in the wave vector domain. (i)–(l) The corresponding total acoustic pressure distributions.

Figure 1 shows the basic principle of the above idea to create acoustic illusions. Assuming we consider two objects: a fish with its acoustic scattering potential $V_1(x, y)$ [defined in Eq. (3)] in Fig. 1(a), and a squid with its acoustic scattering potential $V_2(x, y)$ in Fig. 1(f). In the wave vector domain, their Fourier components can be denoted by $V_1(k_x, k_y)$ and $V_2(k_x, k_y)$ in Figs. 1(b) and 1(g), respectively. From Eq. (8), we know that for a plane wave with an incident direction of $\mathbf{k}_i$, the amplitude of the scattered wave $f(\mathbf{k}_i, \mathbf{k}_s) = V(\mathbf{k}_s - \mathbf{k}_i)$ can be denoted as a circle with its center at $(-k_{i_x}, -k_{i_y})$ and a radius of k_i. For a frequency band, e.g., $k_{i0} \sim k_{i1}$, the scattering amplitude can be denoted as a crescent region between two circles with centers of $(-k_{i0_x}, -k_{i0_y})$, $(-k_{i1_x}, -k_{i1_y})$ and radii of k_{i0}, k_{i1}, respectively. The main idea for acoustic illusion is shown in Figs. 1(c) and 1(h), where we exchange the two crescent regions (acoustic scattering potentials) for each other. Therefore, the scattered acoustic pressure distributions for the fish and squid are exchanged. When transformed to the space domain by an inverse Fourier transformation, we find that the acoustic scattering potentials are not significantly changed, i.e., when we touch or see the fish or squid, it is still a fish or squid [shown in Figs. 1(d) and 1(i)]. However, the far-field scattered acoustic pressure distributions [related to $f(\mathbf{k}_i, \mathbf{k}_s)$] are exchanged, i.e., when we detect the scattered acoustic pressure, we find that it changes to a squid or fish [shown in Figs. 1(e) and 1(j)]. Note that we use two symmetrical crescent regions (corresponding to two wave vectors of $\pm\mathbf{k}_i$) in Fig. 1 to ensure the bidirectional illusion effect and also to avoid the imaginary part (no gain or loss) of the acoustic scattering potential (because symmetrical scattering potentials satisfying $V(-k_x, -k_y) = V(k_x, k_y)$ in the wave vector domain would have no imaginary parts after the inverse Fourier transformation).

III. SIMULATION

Example I: Changing one object into another object. In the first example, we use simulations to show how to use the above method to create an acoustic illusion by changing one object into another object. The background

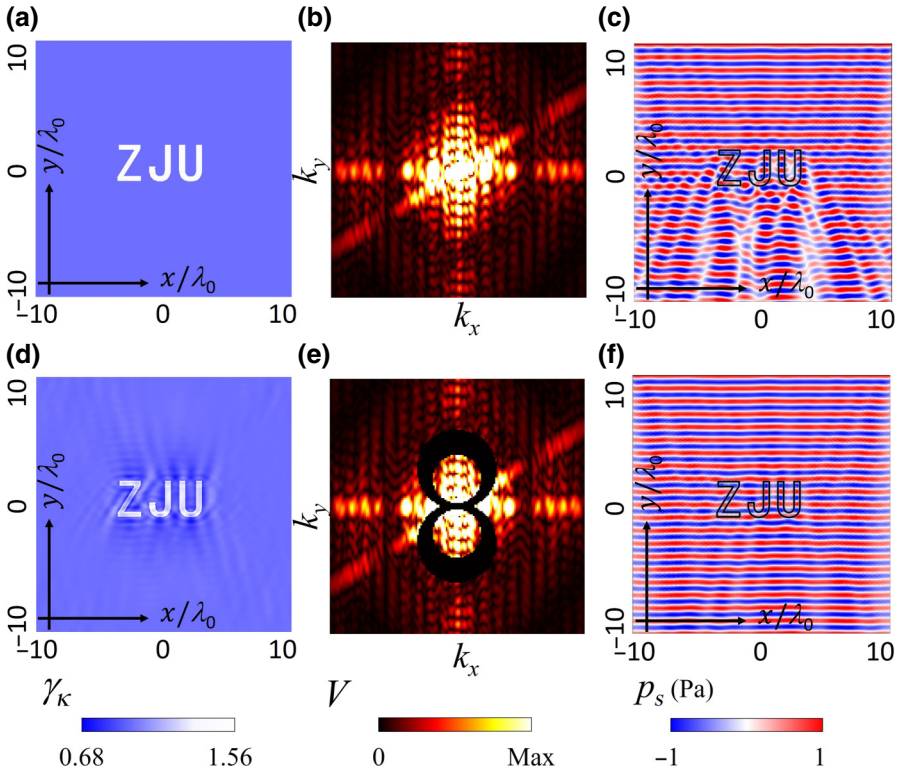

FIG. 3. Acoustic self-cloaking effect. The relative compressibility coefficient of (a) the original object and (d) the modified object. (b),(e) The corresponding acoustic scattering potentials in the wave vector domain. (c),(e) The corresponding total acoustic pressure distributions.

material we use is air (with an acoustic speed of $v_0 = \sqrt{\kappa_0/\rho_0}$). The two objects we choose here are a capsule shape with a length of $6\lambda_0$ and a width of $0.6\lambda_0$ and an isosceles triangle with a base of $1.5\lambda_0$ and height of $3\lambda_0$ ($\lambda_0 = 0.34$ m). These two objects are placed at the central origin of a simulation region (with a size of $20\lambda_0 \times 20\lambda_0$, surrounded by perfect matched layer). For simplicity, we assume the mass density is the same as the background and the relative compressibility coefficient $\gamma_\kappa = V(\boldsymbol{\rho}) + 1$ for the objects and the background are 1.5 and 1, respectively, which are shown in Figs. 2(a) and 2(c). Note that we can also modify the mass density since the key factor determining the scattered acoustic pressure is $V(\boldsymbol{\rho}) = \gamma_\kappa \gamma_\rho - 1$. The corresponding acoustic scattering potentials in the wave vector domain are shown in Figs. 2(e) and 2(g). An incident acoustic plane wave with a wavelength of λ_0 impinges from the top on the objects and results in the total acoustic pressure distributions (p_s) shown in Figs. 2(i) and 2(k). To get the illusion effect, we exchange the two regions of the acoustic scattering potential in the wave vector domain in Figs. 2(e) and 2(g) with each other to form two recombined scattering potentials, shown in Figs. 2(f) and 2(h). The upper part of the two symmetrical regions we choose here is within two circles with centers of $(0, 1.15k_0)$, $(0, 0.85k_0)$ and radii of 1.25 k_0, 0.75 k_0 ($k_0 = 2\pi/\lambda_0$), which correspond to an acoustic wavelength range of $0.80\lambda_0$–$1.33\lambda_0$. The relative compressibility coefficient corresponding to the two recombined scattering potentials in the space domain are shown in Figs. 2(b) and 2(d), where we can see a moderate modification of the original objects. The total acoustic pressure distributions under the same incident wave are shown in Figs. 2(j) and 2(l). We can see that the achieved illusion effects are good: the modified capsule shape [Fig. 2(j)] has the same pressure distributions as the original isosceles triangle [Fig. 2(k)] and the modified isosceles triangle [Fig. 2(l)] has the same pressure distributions as the original capsule shape [Fig. 2(i)]. Therefore, we have changed one object to another object in terms of acoustic detection.

Example II: Acoustic self-cloaking effect.

One specific example of acoustic illusion is acoustic invisibility cloaks. Here, we show an acoustic self-cloaking effect using the above method. The simulation configuration is similar to Example I, and the only difference is the object, which is replaced by three English letters "ZJU" (abbreviation for Zhejiang University). The relative compressibility coefficients of the letters and background are 1.5 and 1, respectively [shown in Fig. 3(a)]. The acoustic scattering potential in the wave vector domain is shown in Fig. 3(b). In order to get a cloaking effect, we set to zero the scattering potential in the two symmetrical regions, whose upper part is within two circles with their centers of $(0, 1.15k_0)$, $(0, 0.85k_0)$ and radii of 1.25 k_0, 0.75 k_0 [see Fig. 3(e)]. The corresponding relative compressibility coefficients are also modified to Fig. 3(d), which can be obtained by an inverse Fourier transform. The total acoustic pressure distributions before and after we modify the acoustic scattering potential are shown in Figs. 3(c) and

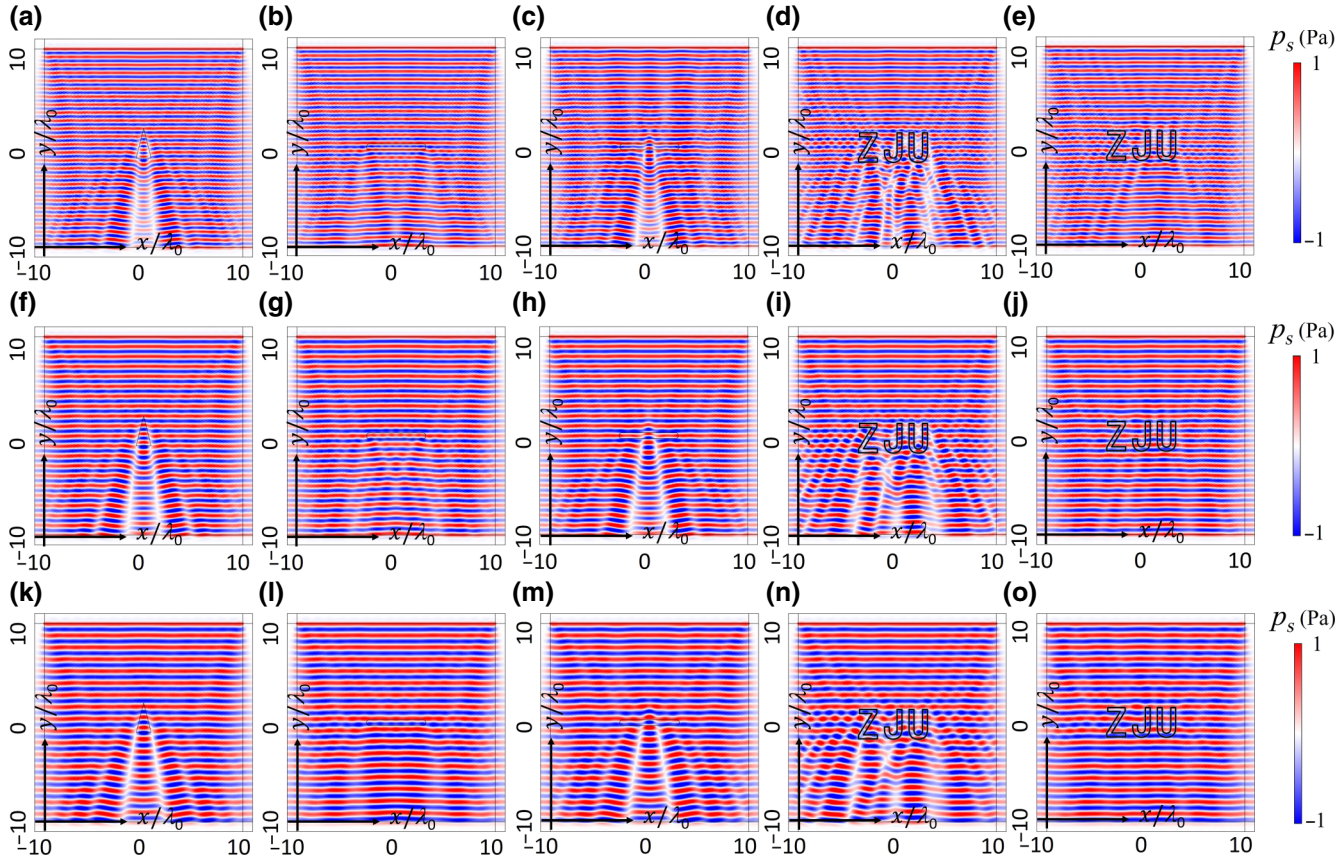

FIG. 4. Total acoustic pressure distributions of the objects in Examples I and II with incident acoustic waves of different frequencies. The three rows represent three wavelengths: (a)–(e) $1.2\boldsymbol{\lambda_0}$, (f)–(j) $1.0\boldsymbol{\lambda_0}$, and (k)–(o) $0.8\boldsymbol{\lambda_0}$. The five columns (from left to right) represent: the original isosceles triangle, the original capsule shape, the modified capsule shape, the original "ZJU," and the modified "ZJU," respectively.

3(f), respectively. We can see that the scattered acoustic waves are greatly suppressed and a good cloaking effect is achieved.

IV. DISCUSSION

We now discuss the bandwidth of the acoustic illusion device and the influence of the direction of the incident acoustic wave. In general, the frequency band can be infinitely large and can work under arbitrary incident directions as long as we make enough modifications to the scattering potential. However, these operations will completely change the object to another object, which will diminish the significance of the illusion. Therefore, the key idea of this method is: for an acoustic detection within a specified frequency band and limited incident angles, we can let the detector get the desired acoustic signal as we do not want to significantly change the original object. We design a kind of illusion device, which has a bidirectional illusion effect within a specified frequency band. Now we use simulations to show the bandwidth and the bidirectional effect. The configuration of the simulation is the same as that of Example I. Figure 4 shows the total acoustic pressure distributions of the objects in Examples I and II under the impinging of three incident acoustic waves at wavelengths of $1.2\lambda_0$, $1.0\lambda_0$, and $0.8\lambda_0$. We can see that good illusion effects remain when the working frequency is within our predesigned frequency band. We also show the bidirectional illusion effects in Fig. 5. Our numerical results for the total acoustic pressure distributions of the objects in Examples I and II show good illusion effects for incident plane waves from the top and the bottom.

Here, we show how to design an illusion device working under a point source. The objects are the same as in Example I, and the only difference is that the plane wave is changed to a point source, which is placed at $x = -3\lambda_0$, $y = 6\lambda_0$ (shown in Fig. 6). For a point source, the incident wave vector is no longer a fixed vector, but covers a range of directions, e.g., from $\pi/2$ to $3\pi/4$ in this case. Therefore, in this case, we should modify a larger region as shown in the inset of Fig. 6(d), e.g., we rotate the two crescent regions anticlockwise in Fig. 2(f) by 45° so that the whole k region from $\pi/2$ to $3\pi/4$ will be covered. The relative compressibility coefficient is shown in

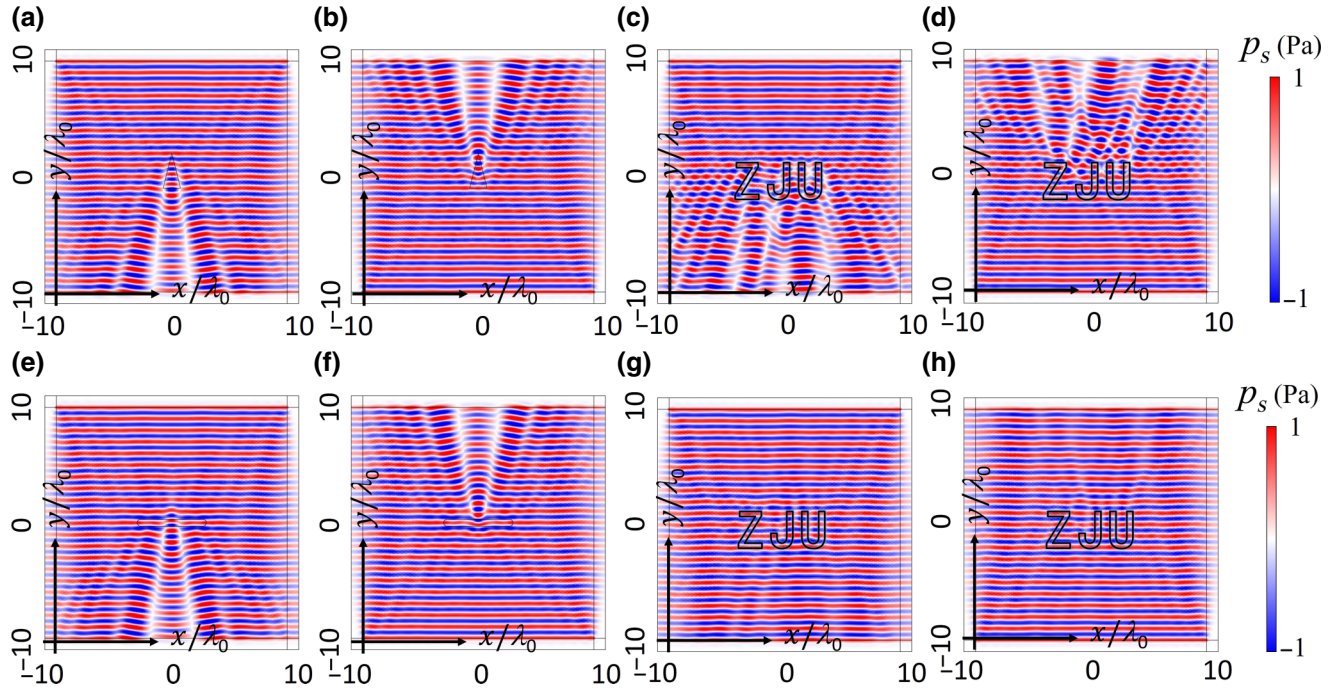

FIG. 5. Total acoustic pressure distributions with different incident directions. Scattering patterns of (a),(b) the original isosceles triangle, (c),(d) the original "ZJU," (e),(f) the modified capsule shape, and (g),(h) the modified "ZJU," under impinging from ((a),(c),(e),(g)) the top and ((b),(d),(f),(h)) the bottom.

Fig. 6(d). Fortunately, this further modification does not change much of the relative compressibility coefficient in Fig. 6(c). The distributions of the total acoustic pressure amplitude are shown in Figs. 6(e)–6(h), corresponding to the capsule shape, the triangle, the modified capsule shape for a bidirectional illusion, and the modified capsule shape for a point source illusion, respectively. We can see that the compressibility coefficient distributions of Figs. 6(d) and 6(b) give similar scattering patterns in Figs. 6(h) and 6(f), while the compressibility coefficient distribution of Fig. 6(c) gives different scattering [Fig. 6(g)]. This verifies our illusion design for a point source.

From the theory and simulation parts, we know that the illusion device is infinitely extended in space. However, we can truncate it at a proper boundary as long as the relative compressibility coefficient outside the boundary is very close to 1. Such a truncation is the same for cloaking and illusion. Figure 7 shows the truncated illusion device (using the sample in Example II). Figure 7(a)–7(d) represent the original self-cloaking device, the truncated device with a circle (with a radius of $6\lambda_0$), the truncated device with a smaller circle (with a radius of $4\lambda_0$), and the original object without a cloak, respectively. We can see from Figs. 7(e)–7(g) that the truncated cloaks still have good performance. This is because almost all of the major modifications occur near the object, and the modifications in the far region are very small and consequently have negligible contributions to the illusion effect.

Note although both our method and the conformal mapping $w = 1/z$ have similar crescent regions, the crescent regions in the present paper represent a k region (or frequency region), while in conformal transformation optics, the crescent region usually represents a deformed space region at a fixed frequency. Therefore, we cannot make a similar design using conformal transformation optics [24].

V. UNDERWATER ACOUSTIC ILLUSION WITH NATURAL MATERIALS

Before we conclude, we discuss some potential applications of the proposed method in this section. One potential application is for underwater illusions. The acoustic velocity in gasoline ($v_1 = 1250$ m/s) is smaller than that in water ($v_b = 1482$ m/s), and thus a special shape of gasoline in water can be detected using acoustic waves. Now we show how to change a capsule shape of gasoline to a triangle shape by using only two natural materials: gasoline and linseed oil ($v_2 = 1770$ m/s). The acoustic scattering potential can be rewritten as

$$V(\boldsymbol{\rho}) = \frac{1}{v_r^2} - 1, \tag{9}$$

where v_r is the relative velocity defined by $v_r = v/v_b$. Figures 8(a) and 8(b) show the original capsule shape and

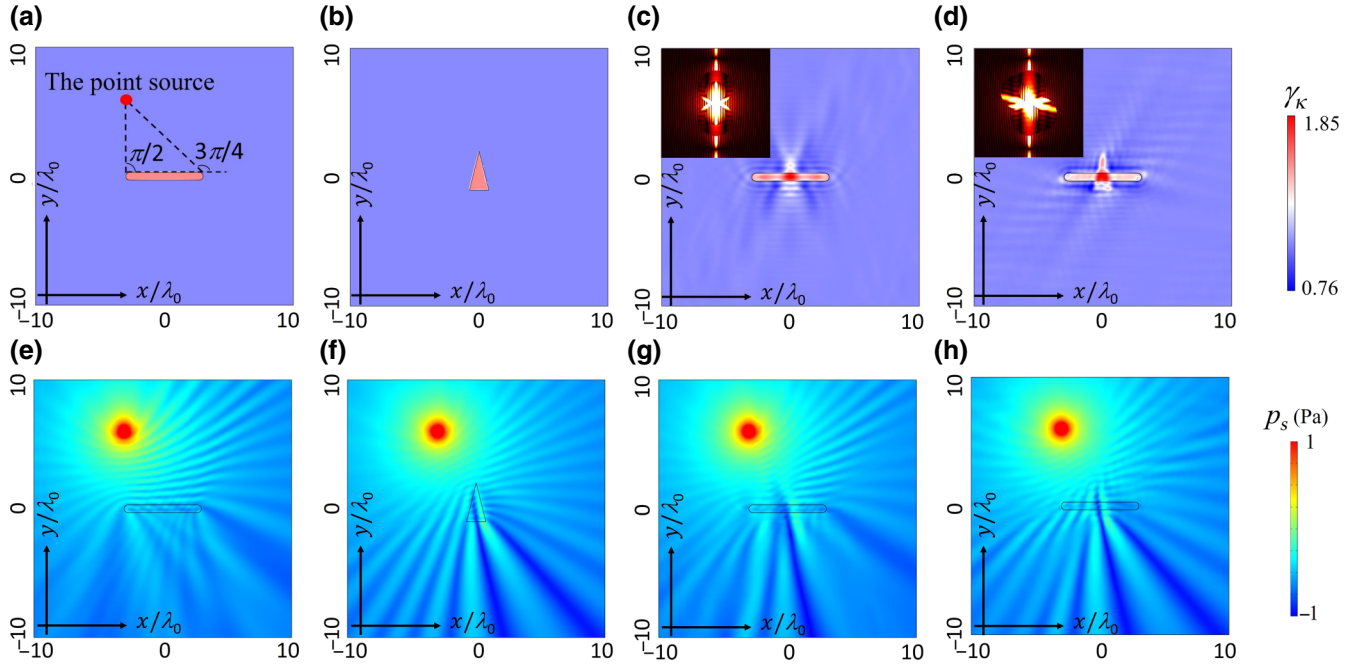

FIG. 6. The case of a point source. The relative compressibility coefficient of (a) the original capsule shape, (b) the original isosceles triangle, (c) the modified capsule shape for bidirectional illusion, and (d) the modified capsule shape for a point source illusion. (e)–(h) The corresponding amplitudes of the total acoustic pressure.

triangle with a scattering potential of $V = 0.2$. We can easily obtain the scattering potential of the modified capsule (with the same scattering pattern as the triangle) using the same method as in Example I. We find the scattering potential of the modified capsule range to be -0.09 to 0.34. These values can be realized using the effective medium theory. We use unit cells with side lengths of $1/5\lambda_0$. The gasoline or linseed oil is filled inside a square with a side

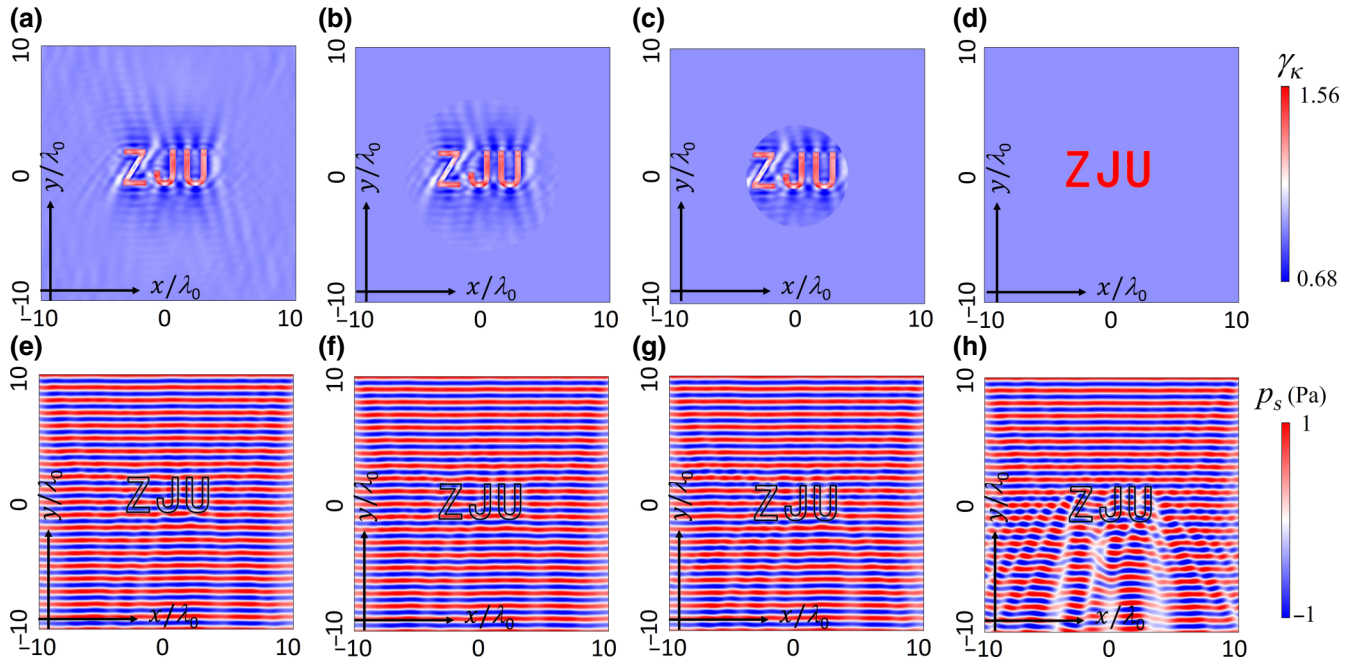

FIG. 7. (a)–(d) The relative compressibility coefficient and (e)–(h) the total acoustic pressure distributions for the original self-cloaking device and the truncated ones. (a) The original self-cloaking device. (b) Truncated radius of $6\lambda_0$. (c) Truncated radius of $4\lambda_0$. (d) Original object without cloak.

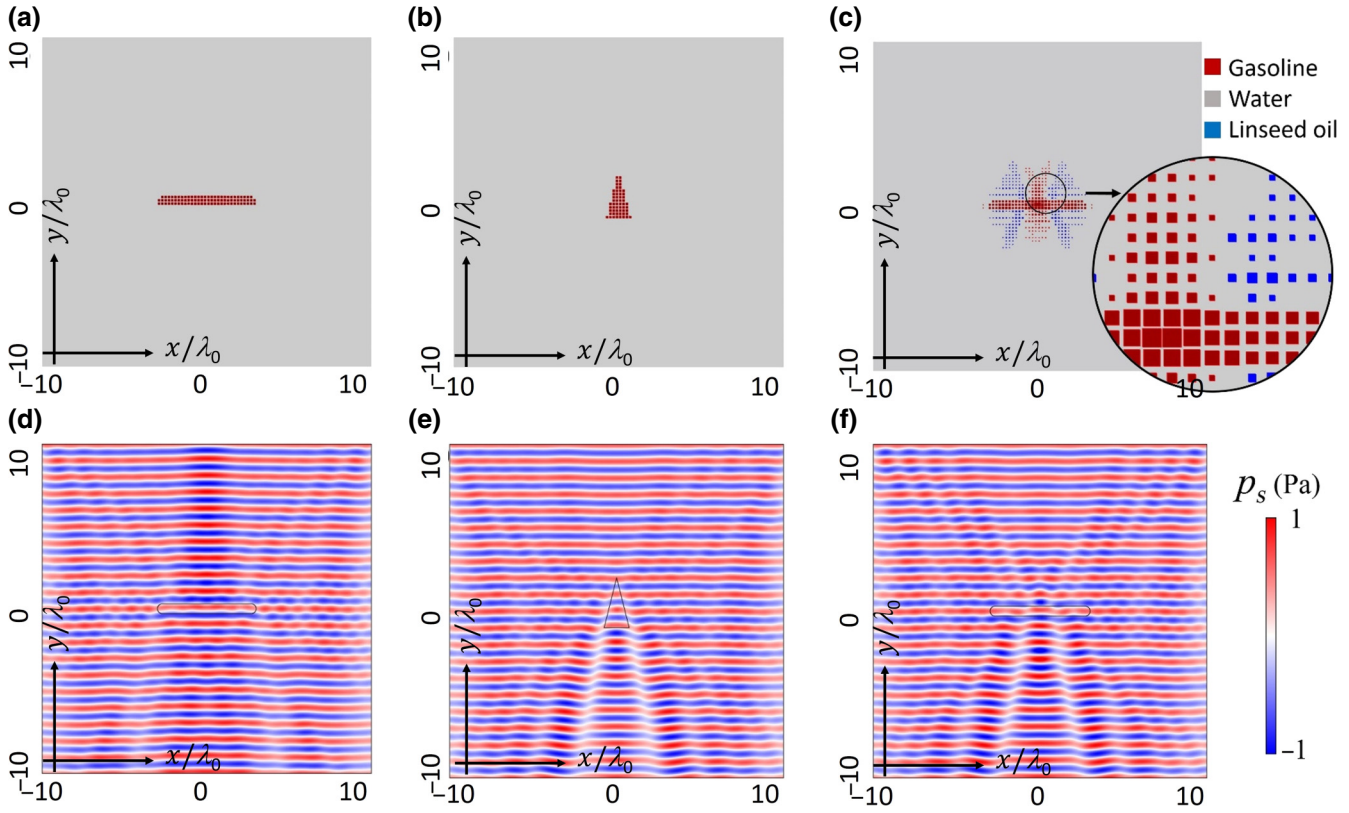

FIG. 8. (a)–(c) The unit cell structures of the original objects: (a) capsule shape, (b) triangle shape, and (c) the modified capsule shape. (d)–(f) The corresponding total acoustic pressure distributions.

length of $1/5\lambda_0 f$ (f is the filling factor) and the remaining part is filled with water. The effective scattering potential can be calculated as

$$V_{\text{eff}} = f^2 V, \tag{10}$$

where V is the scattering potential of gasoline or linseed oil. Note that in the above formula, we have dropped $+(1-f^2)V_{\text{water}}$ because $V_{\text{water}} = 0$. The scattering potentials for gasoline and linseed oil are 0.406 and −0.300, respectively, which can be easily obtained from Eq. (9). Using the effective medium theory, i.e., Eq. (10), we can easily construct the unit cell of the modified capsule shape, i.e., determine the filling factor (we neglect some unit cell structures when f is too small), which is shown in Fig. 8(c). A detailed structure is given in the inset. We can see that although the modified scattering potential extends to the whole space in Fig. 2(b), in real applications, it can be truncated to a small region, as shown in Fig. 8(c). Figures 8(d)–8(f) are the corresponding total acoustic pressure distributions from which we can clearly see a good illusion effect.

VI. CONCLUSION

Our method can be extended for em waves by using the refractive index to represent the scattering potential. For elastic waves, when we neglect the coupling between different wave types, we can obtain a similar differential equation for longitudinal or transversal waves, then we can adopt a similar method to design illusion devises for elastic and seismic waves. In conclusion, we have developed a method to design acoustic illusion devices by manipulating the acoustic scattering potential in the wave vector domain. This method greatly simplifies the material parameters compared with the method of TO and puts illusion devices one step closer to real applications. Our method could pave the way for the design of modern acoustic illusion devices (including camouflage for antisonar detection).

ACKNOWLEDGMENTS

This work was partially supported by the National Natural Science Foundation of China (Grants No. 11604292, No. 11621101, No. 91233208, and No. 60990322), the Postdoctoral Science Foundation of China (Grant No. 2018M632455), the National Key Research and Development Program of China (Grant No. 2017YFA0205700), the fundamental research funds for the central universities (Grant No. 2017FZA5001), and the Program of Zhejiang Leading Team of Science and Technology Innovation, and AOARD.

[1] J. B. Pendry, D. Schurig, and D. R. Smith, Controlling electromagnetic fields, Science **312**, 1780 (2006).

[2] U. Leonhardt, Optical conformal mapping, Science **312**, 1777 (2006).

[3] C. Jiang and X. Zang, Overlapped optics, illusion optics, and an external cloak based on shifting media, J. Opt. Soc. Am. **28**, 1994 (2011).

[4] X. Zang, C. Shi, Z. Li, L. Chen, B. Cai, Y. Zhu, and H. Zhu, Illusion induced overlapped optics, Opt. Express **22**, 582 (2014).

[5] Y. Lai, J. Ng, H. Chen, D. Han, J. Xiao, Z. Q. Zhang, and C. T. Chan, Illusion Optics: The Optical Transformation of an Object Into Another Object, Phys. Rev. Lett. **102**, 253902 (2009).

[6] W. S. Cai, U. K. Chettiar, A. V. Kildishev, and V. M. Shalaev, Optical cloaking with metamaterials, Nat. Photonics **1**, 224 (2007).

[7] T. Ergin, N. Stenger, P. Brenner, J. B. Pendry, and M. Wegener, Three-dimensional invisibility cloak at optical wavelengths, Science **328**, 337 (2010).

[8] L. H. Gabrielli, J. Cardenas, C. B. Poitras, and M. Lipson, Silicon nanostructure cloak operating at optical frequencies, Nat. Photonics **3**, 461 (2009).

[9] J. S. Li and J. B. Pendry, Hiding Under the Carpet: A New Strategy for Cloaking, Phys. Rev. Lett. **101**, 203901 (2008).

[10] R. Liu, C. Ji, J. J. Mock, J. Y. Chin, T. J. Cui, and D. R. Smith, Broadband ground-plane cloak, Science **323**, 366 (2009).

[11] B. Zhang, Y. Luo, X. Liu, and G. Barbastathis, Macroscopic Invisibility Cloak for Visible Light, Phys. Rev. Lett. **106**, 033901 (2011).

[12] D. Schurig, J. J. Mock, B. J. Justice, S. A. Cummer, J. B. Pendry, A. F. Starr, and D. R. Smith, Metamaterial electromagnetic cloak at microwave frequencies, Science **314**, 977 (2006).

[13] M. Yan, W. Yan, and M. Qiu, Cylindrical superlens by a coordinate transformation, Phys. Rev. B **78**, 125113 (2008).

[14] M. Tsang and D. Psaltis, Magnifying perfect lens and superlens design by coordinate transformation, Phys. Rev. B **77**, 035122 (2008).

[15] J. B. Pendry, Negative Refraction Makes a Perfect Lens, Phys. Rev. Lett. **85**, 3966 (2000).

[16] Y. Luo, H. S. Chen, J. J. Zhang, L. X. Ran, and J. A. Kong, Design and analytical full-wave validation of the invisibility cloaks, concentrators, and field rotators created with a general class of transformations, Phys. Rev. B **77**, 125127 (2008).

[17] W. X. Jiang, T. J. Cui, Q. Cheng, J. Y. Chin, X. M. Yang, R. P. Liu, and D. R. Smith, Design of arbitrarily shaped concentrators based on conformally optical transformation of nonuniform rational B-spline surfaces, Appl. Phys. Lett. **92**, 264101 (2008).

[18] M. Rahm, D. Schurig, D. A. Roberts, S. A. Cummer, D. R. Smith, and J. B. Pendry, Design of electromagnetic cloaks and concentrators using form-invariant coordinate transformations of Maxwell's equations, Photonic. Nanostruct. **6**, 87 (2008).

[19] H. Chen, B. Hou, S. Chen, X. Ao, W. Wen, and C. T. Chan, Design and Experimental Realization of a Broadband Transformation Media Field Rotator at Microwave Frequencies, Phys. Rev. Lett. **102**, 183903 (2009).

[20] Y. Xu, S. Du, L. Gao, and H. Chen, Overlapped illusion optics: a perfect lens brings a brighter feature, New J. Phys. **13**, 262 (2011).

[21] C. Li, X. Meng, X. Liu, F. Li, G. Fang, H. Chen, and C. T. Chan, Experimental Realization of a Circuit-Based Broadband Illusion-Optics Analogue, Phys. Rev. Lett. **105**, 233906 (2010).

[22] H. R. Shoorian and M. S. Abrishamian, Design of optical switches by illusion optics, J. Opt. **15**, 527 (2013).

[23] J. J. Li, X. F. Zang, J. F. Mao, M. Tang, Y. M. Zhu, and S. L. Zhuang, Overlapped optics induced perfect coherent effects, Sci. Rep. **3**, 3569 (2013).

[24] L. Xu and H. Chen, Conformal transformation optics, Nat. Photonics **9**, 15 (2015).

[25] R. Fleury, F. Monticone, and A. Alù, Invisibility and Cloaking: Origins, Present, and Future Perspectives, Phys. Rev. Appl. **4**, 037001 (2015).

[26] F. Sun, B. Zheng, H. Chen, W. Jiang, S. Guo, Y. Liu, Y. Ma, and S. He, Transformation Optics: From Classic Theory and Applications to its New Branches, Laser Photonics Rev. **11**, 1700034 (2017).

[27] H. Chen and C. T. Chan, Acoustic cloaking in three dimensions using acoustic metamaterials, Appl. Phys. Lett. **91**, 45 (2007).

[28] D. Torrent and J. Sánchezdehesa, Acoustic cloaking in two dimensions: a feasible approach, New J. Phys. **10**, 063015 (2008).

[29] S. Zhang, C. Xia, and N. Fang, Broadband Acoustic Cloak for Ultrasound Waves, Phys. Rev. Lett. **106**, 024301 (2011).

[30] Q. Wei, Y. Cheng, and X. Liu, Negative refraction induced acoustic concentrator and the effects of scattering cancellation, imaging, and mirage, Phys. Rev. B **86**, 499 (2012).

[31] X. Jiang, B. Liang, X. Y. Zou, L. L. Yin, and J. C. Cheng, Broadband field rotator based on acoustic metamaterials, Appl. Phys. Lett. **104**, 1780 (2014).

[32] W. Kan, B. Liang, X. Zhu, R. Li, X. Zou, H. Wu, J. Yang, and J. Cheng, Acoustic illusion near boundaries of arbitrary curved geometry, Sci. Rep. **3**, 1427 (2013).

[33] W. Kan, B. Liang, R. Li, X. Jiang, X. Y. Zou, L. L. Yin, and J. Cheng, Three-dimensional broadband acoustic illusion cloak for sound-hard boundaries of curved geometry, Sci. Rep. **6**, 36936 (2016).

[34] L. Sanchis, V. M. Garcíachocano, R. Llopispontiveros, A. Climente, J. Martínezpastor, F. Cervera, and J. Sánchezdehesa, Three-Dimensional Axisymmetric Cloak Based on the Cancellation of Acoustic Scattering From a Sphere, Phys. Rev. Lett. **110**, 124301 (2013).

[35] M. D. Guild, A. J. Hicks, M. R. Haberman, A. Alù, and P. S. Wilson, Acoustic scattering cancellation of irregular objects surrounded by spherical layers in the resonant regime, J. Appl. Phys. **118**, 016623 (2015).

[36] T. P. Martin, C. A. Rohde, M. D. Guild, C. J. Naify, D. C. Calvo, and G. J. Orris, Acoustic Scattering Cancellation: an Alternative to Coordinate Transformation Scattering Reduction, J. Acoust. Soc. Am. **139**, 2183 (2016).

[37] H. Chen, Y. Zhou, M. Zhou, L. Xu, and Q. H. Liu, Perfect Undetectable Acoustic Device from Fabry-Pérot Resonances, Phys. Rev. Appl. **9**, 024014 (2018).

[38] S. A. R. Horsley, M. Artoni, and G. C. L. Rocca, Spatial Kramers–Kronig relations and the reflection of waves, Nat. Photonics **9**, 436 (2015).

[39] D. Ye, C. Cao, T. Zhou, J. Huangfu, G. Zheng, and L. Ran, Observation of reflectionless absorption due to spatial Kramers–Kronig profile, Nat. Commun. **8**, 51 (2017).

[40] W. Jiang, Y. Ma, J. Yuan, G. Yin, W. Wu, and S. He, Deformable broadband metamaterial absorbers engineered with an analytical spatial Kramers-Kronig permittivity profile, Laser Photonics Rev. **11**, 1600253 (2016).

[41] F. Loran and A. Mostafazadeh, Perfect broadband invisibility in isotropic media with gain and loss, Opt. Lett. **42**, 5250 (2017).